# An Optically Transparent Wideband High Impedance Surface

Mahmoud M. Mostafa, Mohamed I. Ibrahim,
and Amr M.E. Safwat
Electronics and Electrical Communication Eng. Department
Faculty of Engineering, Ain Shams University
Cairo, Egypt
mahmoud.mabrouk@eng.asu.edu.eg

Tamer M. Abuelfadl
Electronics and Electrical Communication Department
Faculty of Engineering, Cairo University
Cairo, Egypt

***Abstract*—This paper presents an optically transparent wideband High Impedance Surface (HIS) at 5 GHz. The surface is designed on acrylic substrate. Results show a good matching between the proposed circuit model, EM simulations, and measurements. The ±90° BW is 1 GHz (from 4.5 to 5.5 GHz) and the optical transparency is 80 %.**

***Keywords—high impedance surface; optically transparent***

## I. INTRODUCTION

High impedance surfaces have been extensively used in many applications among them are: low profile high gain antennas [1,2], Electromagnetic Band Gaps (EBGs) [3] and electromagnetic absorbers [4]. Recently, research has been conducted to study optically transparent microwave structures such as absorbers [4], transparent antennas [5, 6], and transparent electric surfaces acting as ground planes [7, 8] for automotive or solar cell applications.

In this paper, an optically transparent high impedance surface using cross and cross loaded loop resonators at 5 GHz is presented. The surface is suitable for WLAN applications with wideband performance. It is characterized by ±90° BW of about 1 GHz and high optical transparency (around 80 %). The theory and design of the surface are presented. Measurement results of the fabricated structure are in a good agreement with the simulated ones.

## II. THEORY

HIS is an artificial surface that provides almost full reflection with magnitude of nearly 0 dB and phase of 0° [9]. A conventional HIS consists of a capacitive patches layer in shunt with a grounded substrate as shown in Fig. 1(a). Its equivalent circuit model is shown in Fig. 1(b). The patch layer acts as a shunt capacitance to the equivalent inductance of the short circuited substrate, so the whole surface acts as a parallel resonance circuit that becomes an open circuit at a certain frequency.

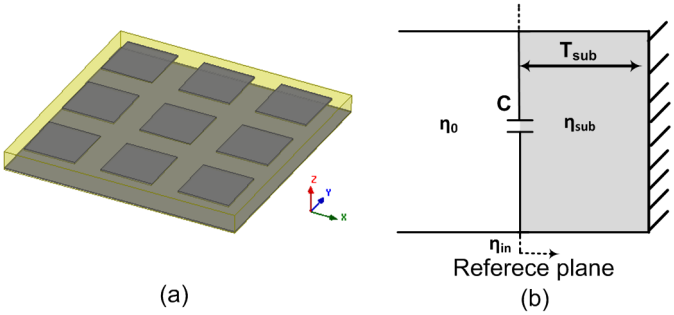


Fig. 1: (a) Conventional HIS unit cell and (b) its circuit model.

The proposed HIS replaces both the ground plane and patch layer with elements that act as series resonators as shown in Fig. 2, where the elements ($L_1$, $C_1$) on one side (lower surface) resonate at $f_1$ and ($L_2$, $C_2$) on the other side (upper surface) resonate at $f_2$. The resonators are designed such that $f_1$ and $f_2$ are close to each other, so that the reflection response of the lower resonator overlaps with the upper one to get a wideband high reflection. $f_1$ is chosen to be lower than $f_2$ and the reference plane is taken on the side corresponding to the resonance $f_2$ as shown in Fig. 2(b). Between $f_1$ and $f_2$ there is a frequency ($f_0$) where ($L_2$, $C_2$) resonator is capacitive and the input impedance seen from the substrate terminated by the ($L_1$, $C_1$) resonator is inductive. At this frequency ($f_0$) parallel resonance is obtained and the surface acts as a high impedance one. Since the reflection phase is 180° at $f_2$, the ±90° BW around $f_0$ is narrow if $f_0$ is close to $f_2$, so the optimum value of $f_0$ is close to $f_1$ and larger than it.

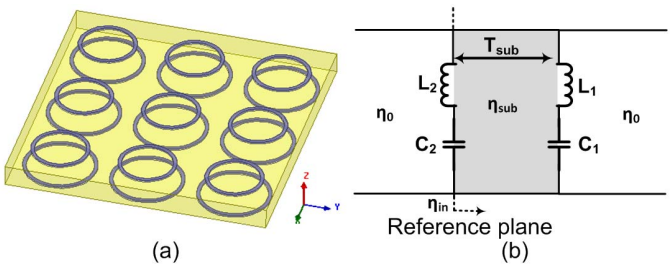


Fig. 2: Proposed design: (a) initial version of lower and upper resonators and (b) the equivalent circuit model of the structure.

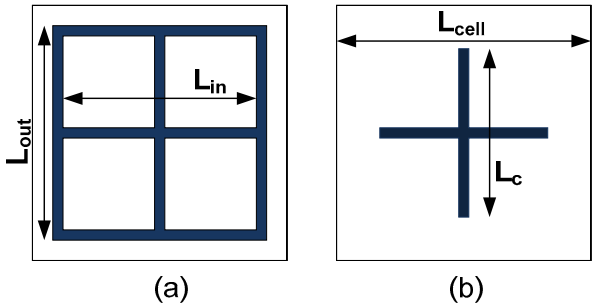


Fig. 3: (a) Proposed unit cell bottom layer and (b) its upper layer.

From circuit simulations, to have $f_0$ = 5 GHz the upper resonator should resonate above 5 GHz while maintaining a low capacitance, i.e. a relatively high inductance is required and a narrow bandwidth is obtained. In order to have an overlap between the lower and upper resonators responses, the lower resonator should have a very high bandwidth (i.e. high capacitance and relatively low inductance). Aligning with these constraints, the lower resonator is designed to be a square loop with two perpendicular wires across it "cross loaded loop or window resonator" [8], and the upper resonator is a simple cross as shown in Fig. 3.

## III. Proposed HIS Design

### A. Acrylic Characterization

In order to define the acrylic relative permittivity ($\varepsilon_r$), which ranges typically from 2 to 4, a coplanar waveguide (CPW) is fabricated on FR4 with $Z_0$ = 100 Ω. The transmission line is terminated with 50 Ohm to resonate at $\lambda_g/2$, where $\lambda_g$ is the guided wavelength. This resonance frequency changes with the effective permittivity of the CPW. Two cases are compared, CPW left in air as shown in Fig. 4(a), and another one with acrylic superstrate as shown in Fig. 4(b). From the change in the resonance frequency between the two cases, $\epsilon_r$ is determined by comparing measurements and EM simulations. The simulated and measured $|S_{11}|$ with acrylic superstrate are shown in Fig. 5. The extracted value of the acrylic relative permittivity is 2.2.

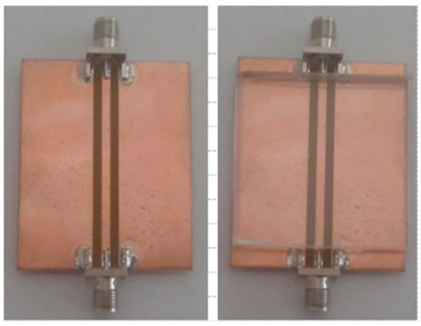


Fig. 4: Fabricated CPW with (a) air superstrate and (b) acrylic superstrate.

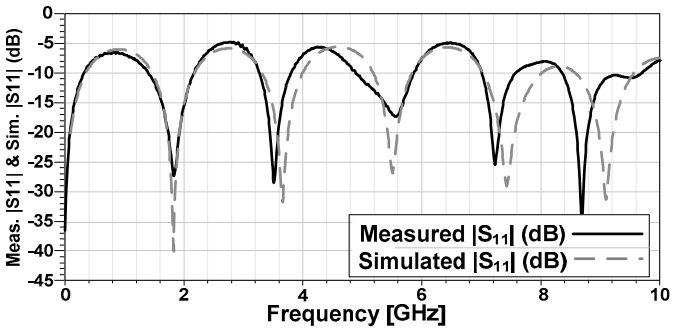


Fig. 5: Measured vs. simulated $|S_{11}|$ of CPW with acrylic superstrate.

### B. Proposed Unit Cell Simulations

Unit cell simulations with Periodic Boundary Conditions (PBCs) are conducted using the commercial EM simulator ANSYS HFSS v15. The bottom and upper layers are copper with thickness of 0.5 mm and trace width of 1 mm, while the substrate is acrylic, which is an optically transparent substrate with thickness of 6 mm and relative permittivity $\epsilon_r$ of 2.2. The copper elements are totally embedded into the substrate. The unit cell length and width ($L_{cell}$) is 25 mm (Fig. 3) which is less than λ/2 to prevent any undesired grating lobes [10], the unit cell simulation setup is shown in Fig. 6. The lower resonator unit cells consist of loops with narrow gaps between each other, and loaded with cross wires ($L_{out}$=21 mm and $L_{in}$=19 mm). The upper unit cells are implemented as simple cross resonators with wide gaps between each other ($L_c$=16.5 mm).

The magnitude and phase of the reflection coefficient along with the magnitude of the transmission coefficient are shown in Fig. 7. The 0° phase occurs at 5.05 GHz and ± the 90° BW (the shaded area in Fig. 7) extends from 4.45 GHz to 5.52 GHz with reflection magnitude larger than -0.76 dB over the whole 1.07 GHz bandwidth.

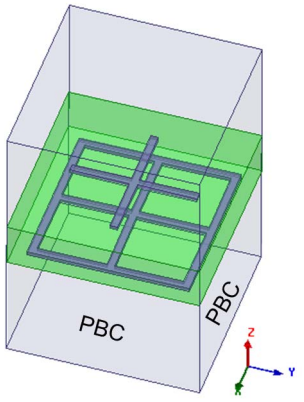


Fig. 6: Proposed unit cell simulation setup.

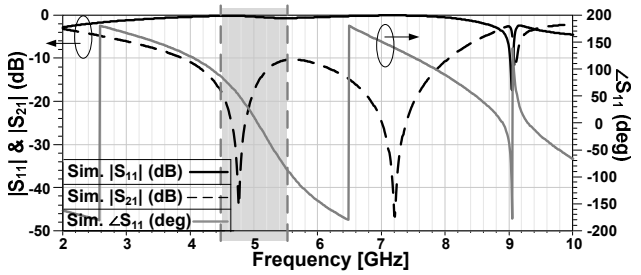


Fig. 7: Unit cell simulated $|S_{11}|$, $|S_{21}|$ and $\angle S_{11}$.

### C. Equivalent Circuit Model

The equivalent transmission line model of the proposed structure is shown in Fig. 8. The values of $L_1$, $C_1$, $L_2$ and $C_2$ are tuned using the commercial circuit simulator ANSYS Designer v8 so that the circuit simulation results match the EM ones. These values are different from those of single resonators as the coupling between the elements isn't considered.

The optimized values are: $L_1$=4.3 nH, $C_1$=260 fF, $L_2$=9.8 nH and $C_2$=50 fF. These values provide close matching between EM and circuit results as shown in Fig. 9. The dip, which occurs in $|S_{11}|$ and $|S_{21}|$ at 9 GHz in EM simulations and does not appear in circuit results, is due to the generation of the first higher order spatial harmonic when $L_{cell}=\lambda_0/\epsilon_{eff}$, where $\lambda_0$ is the free space wavelength at 9 GHz and $\epsilon_{eff}$ is the effective permittivity (between air and acrylic) and it is found to be 1.326 in our case.

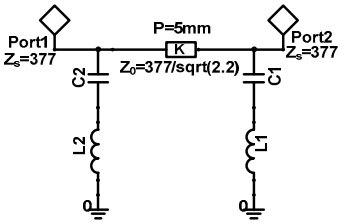


Fig. 8: Proposed structure circuit model.

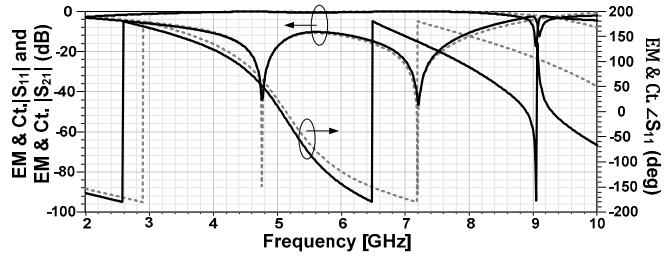


Fig. 9: EM vs. circuit simulation results, EM results are solid lines while circuit results are dotted lines.

## IV. Fabrication and Measurements

### A. Proposed Surface Fabrication

A 12×12 elements surface is fabricated as shown in Fig. 10. A laser cutting machine is used to cut the copper elements from a sheet of 0.5 mm thickness. The acrylic substrate of thickness 6 mm (i.e. $\lambda_0/10$ where $\lambda_0$ is the free space wavelength at 5 GHz) has been periodically engraved using another laser machine resulting in V-shape grooves with same dimensions of the copper elements. The copper elements are put in the grooves and then are held fixed using a transparent tape so that they don't fall during measurement, the optical transparency ($T$) is calculated as follows:

$$T = 1 - (\textit{copper area} / \textit{total unit cell area}) \quad (1)$$

where copper area is the area of the lower window resonator only as the upper resonator is perfectly aligned over the lower one.

### B. Measurement Setups and Results

The measurement setup for the transmission coefficient is shown in Fig. 11. It is composed of two antennas, one in front of the surface to illuminate it, and the other is behind it to measure the received power. The measured transmission coefficient compared to the simulated one is shown in Fig. 12.


Fig. 10: Fabricated proposed HIS.

Fig. 11: Measurement setup of $S_{21}$.

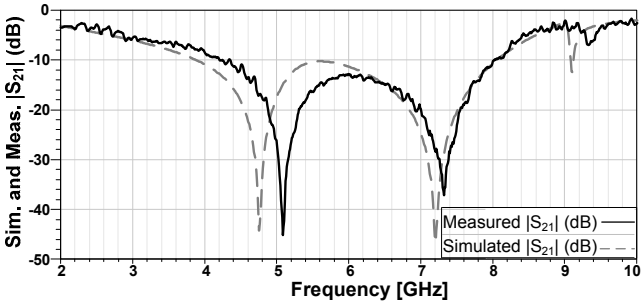


Fig. 12: Simulated vs. measured $|S_{21}|$.

The measurement setup for the reflection coefficient is shown in Fig. 13. It is composed of two antennas, one to illuminate the surface while the other receives the reflected waves. Both antennas are located in front of the surface. The system is calibrated with a metallic sheet placed in front of the two antennas. When the thru calibration step is conducted the metallic sheet determines the location of the reference plane. In the measurement process, the proposed surface is placed at this

reference plane such that the measured $S_{21}$ represents the reflection coefficient with 180° phase shift.

Hence, the phase of the reflection coefficient i s obtained as follows:

$$\angle(S_{11})_{prop.\ surf.} = \angle(S_{11})_{meas.\ surf.} - 180° \quad (2)$$

where $(S_{11})_{meas.\ surf.}$ is the measured reflection coefficient when measuring the fabricated surface. The measured reflection coefficient compared to the simulated one is shown in Fig. 14.

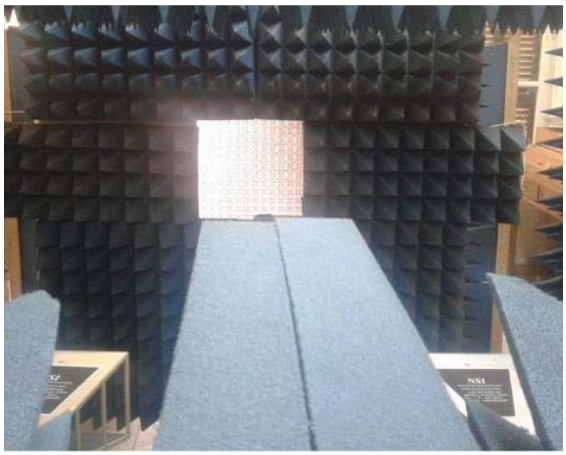

Fig. 13: Measurement setup of $S_{11}$.

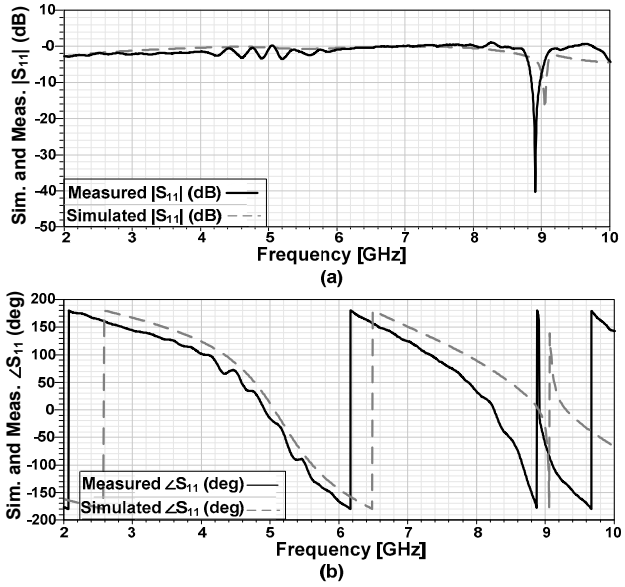


Fig. 14: Simulated vs. measured $S_{11}$ (a) magnitude and (b) phase.

Measurements show that there are shifts in the two resonance frequencies of 300 MHz at $f_1$ and 100 MHz at $f_2$ (Fig. 12). There is also a shift in the HIS frequency $f_0$ of 140 MHz (Fig. 14) and finally there are ripples in the magnitude of the reflection coefficient that range from 0 to -3.5 dB. The discrepancies between the measured and simulated data are due to many reasons, e.g. the inaccuracy in acrylic $\epsilon_r$ measurement, the V-groove shapes –the laser machine couldn't make rectangular grooves– that left air gaps below the copper elements, and the transparent tape used to hold the copper elements.

## V. Conclusion

An optically transparent high impedance surface using cross and cross loaded loop resonators at 5 GHz was presented. The surface is suitable for WLAN applications with wideband performance. It is characterized by ±90° BW of around 1 GHz, high optical transparency (around 80 %) and low profile (surface thickness is around $\lambda_0/10$).The simulated and measured results were in a good agreement.

## Acknowledgment

This project was supported financially by the Science and Technology Development Fund (STDF), Egypt, Grant No. 14933.

## References

[1] M. Ibrahim, S. Elhenawy and A. Safwat, "60 GHz artificial magnetic conductor loaded dipole antenna in 65 nm CMOS technology," in Proc. European Microwave Conference (EuMC), Rome, Italy, Oct. 2014.

[2] H. Kamoda, S. Kitazawa, N. Kukutsu and K. Kobayashi, "Loop Antenna over Artificial Magnetic Conductor Surface and its Application to Dual-Band RF Energy Harvesting," *IEEE Trans. Antennas Propag.*, vol. 63, no. 10, pp. 4408-441, Oct. 2015.

[3] W. Yang, H. Wang, W.Q. Che, Y. Huang and J. Wang, "High-gain and low-loss millimeter-wave LTCC antenna array using artificial magnetic conductor structure," *IEEE Trans. Antennas Propag.*, vol. 63 no. 1, pp. 390-395, Jan. 2015.

[4] Y. Okano, S. Ogino and K. Ishikawa, "Development of Optically Transparent Ultrathin Microwave Absorber for Ultrahigh-Frequency RF Identification System," *IEEE Trans. Microw. Theory Tech.*, vol. 60 no. 8, pp. 2456-2464, Aug. 2012.

[5] E.R. Escobar, N.J. Kirsch, G. Kontopidis and B. Turner, "5.5 GHz optically transparent mesh wire microstrip patch antenna," *IET Electronics Letters*, vol. 51 no. 16, pp. 1220-1222, Aug. 2015.

[6] A. Martin, X. Castel, O. Lafond and M. Himdi, "Optically transparent frequency-agile antenna for X-band applications," *IET Electronics Letters*, vol. 51 no. 16, pp. 1231-1233, Aug. 2015.

[7] M. Kashanianfard and K. Sarabandi, "Metamaterial inspired optically transparent band selective ground planes for antenna applications," *IEEE Trans. Antennas Propag.*, vol. 61 no. 9, pp. 4624-4631, Sept. 2013.

[8] M. Kashanianfard and K. Sarabandi, "Transparent ground planes for automotive applications," in Proc. Antennas and Propagation in Wireless Communications (APWC), Palm Beach, USA, Aug. 2014.

[9] D. Sievenpiper, L. Zhang, R.F.J. Broas, N.G. Alexopolous and E. Yablonovitch, "High impedance electromagnetic surfaces with a forbidden frequency band," *IEEE Trans. Microw. Theory Tech.*, vol. 47 no. 11, pp. 2059-2074, Nov. 1999.

[10] B.A. Munk, Frequency selective surfaces: Theory and design,New York: Wiley, 2000, pp. 23-25.